Molecular Cancer Therapeutics

Mechanisms of Pinometostat (EPZ-5676) Treatment–Emergent Resistance in *MLL*-Rearranged Leukemia

Carly T. Campbell[1], Jessica N. Haladyna[2], David A. Drubin[3], Ty M. Thomson[3], Michael J. Maria[3], Taylor Yamauchi[2], Nigel J. Waters[1], Edward J. Olhava[1], Roy M. Pollock[1], Jesse J. Smith[1], Robert A. Copeland[1], Stephen J. Blakemore[1], Kathrin M. Bernt[4], and Scott R. Daigle[1]

Abstract

DOT1L is a protein methyltransferase involved in the development and maintenance of *MLL*-rearranged (*MLL*-r) leukemia through its ectopic methylation of histones associated with well-characterized leukemic genes. Pinometostat (EPZ-5676), a selective inhibitor of DOT1L, is in clinical development in relapsed/refractory acute leukemia patients harboring rearrangements of the *MLL* gene. The observation of responses and subsequent relapses in the adult trial treating *MLL*-r patients motivated preclinical investigations into potential mechanisms of pinometostat treatment-emergent resistance (TER) in cell lines confirmed to have *MLL*-r. TER was achieved in five *MLL*-r cell lines, KOPN-8, MOLM-13, MV4-11, NOMO-1, and SEM. Two of the cell lines, KOPN-8 and NOMO-1, were thoroughly characterized to understand the mechanisms involved in pinometostat resistance. Unlike many other targeted therapies, resistance does not appear to be achieved through drug-induced selection of mutations of the target itself. Instead, we identified both drug efflux transporter dependent and independent mechanisms of resistance to pinometostat. In KOPN-8 TER cells, increased expression of the drug efflux transporter ABCB1 (P-glycoprotein, MDR1) was the primary mechanism of drug resistance. In contrast, resistance in NOMO-1 cells occurs through a mechanism other than upregulation of a specific efflux pump. RNA-seq analysis performed on both parental and resistant KOPN-8 and NOMO-1 cell lines supported two unique candidate pathway mechanisms that may explain the pinometostat resistance observed in these cell lines. These results are the first demonstration of TER models of the DOT1L inhibitor pinometostat and may provide useful tools for investigating clinical resistance. *Mol Cancer Ther; 16(8); 1669–79. ©2017 AACR.*

Introduction

Rearrangements at the 11q23 locus target the gene *MLL* (*KMT2A*), resulting in the oncogenic fusion of the amino terminus of MLL, fused in frame with any of more than 70 fusion partners (1–5). *MLL*-rearrangements (*MLL*-r) occur in 5% to 10% of acute leukemias of lymphoid, myeloid, or mixed phenotype lineage and are especially common in infant acute leukemias (1, 2, 5). Common MLL oncogenic fusion partners include members of the AF and ENL protein families (1–5). Translocations of the *MLL* gene typically involve the loss of the carboxy terminal portion of the MLL protein that contains the SET domain responsible for its methyltransferase activity (1, 2, 5–7). The resulting fusion protein maintains its ability to bind a set of developmentally important genes such as *HOXA9* and *MEIS1* while gaining a fusion partner capable of recruiting DOT1L to a complex that promotes transcriptional elongation (8–17). DOT1L is a protein methyltransferase (PMT) responsible for catalyzing all three methylation states (mono, di, and tri) of lysine 79 on histone H3 (H3K79; ref. 18, 19). The fusion present in *MLL*-r patients leads to the aberrant localization of the DOT1L-containing multi-subunit complex within chromatin followed by the ectopic methylation of H3K79 and enhanced gene expression of leukemogenic genes (9–11, 13, 20). Recent studies involving genetic knockdown and pharmacologic inhibition of DOT1L support the hypothesis that DOT1L drives leukemogenesis through overexpression of *MLL*-r target genes, including *HOXA9* and *MEIS1* (10, 11, 21–24).

Pinometostat (EPZ-5676) is a small molecule inhibitor of DOT1L currently in clinical development for both adult and pediatric relapsed/refractory acute leukemia patients harboring *MLL*-r. Preclinical *in vitro* and *in vivo* studies conducted with pinometostat using models of *MLL*-r demonstrated robust single-agent antiproliferative activity as a direct consequence of pinometostat's selective inhibition of H3K79 methylation and resultant transcriptional repression of *MLL*-r target genes *HOXA9* and *MEIS1* (25). Early reports from the adult phase I clinical trial described responses in *MLL*-r patients, including complete remissions, with subsequent disease progression which motivated preclinical investigation into mechanisms precipitating pinometostat treatment-induced resistance (26).

[1]Epizyme Inc., Cambridge, Massachusetts. [2]University of Colorado Denver, Denver, Colorado. [3]Selventa, Cambridge, Massachusetts. [4]Children's Hospital of Philadelphia, Philadelphia, Pennsylvania.

Note: Supplementary data for this article are available at Molecular Cancer Therapeutics Online (http://mct.aacrjournals.org/).

Corresponding Author: Scott R. Daigle, Epizyme, Inc., 400 Technology Square, 4th Floor, Cambridge, MA 02139. Phone: 617-500-0583; Fax: 617-349-0707; E-mail: sdaigle@epizyme.com

doi: 10.1158/1535-7163.MCT-16-0693

Despite advances in understanding the molecular mechanisms of disease and implementation of targeted therapies, a common limiting factor to sustained efficacy in cancer patients is the emergence of resistant clones (27, 28). Resistance has been reported to occur through multiple mechanisms such as transformation of the drug target through genetic variation (indels or single base modifications), overexpression, and alternative signal transduction (28). Knowledge of the mechanisms of drug-induced resistance can lead to insights for combinations and rational small molecule drug design to develop compounds for overcoming drug resistance (29–31). Point mutations within the coding region of the target are a frequent cause for resistance to targeted therapies and have been observed clinically in acute myeloid leukemia (AML) with small molecules such as FMS-like tyrosine kinase-3 (FLT3) inhibitors (32, 33). For example, following treatment with FLT3 inhibitors PKC412, SU5614, and sorafenib, acquired resistance mutations have been identified in tyrosine kinase domains 1 and 2 at residues N676, F691, D835, and Y842 (34). Similar to a mechanism found for FLT3 inhibitors, preclinical studies performed with inhibitors of the PMT Enhancer of zeste homolog 2 (EZH2) demonstrated that one mechanism of drug resistance in this enzyme class is through the acquisition of secondary point mutations; whether such EZH2 resistance-causing mutations are relevant to the clinical situation is not clear at present (35, 36). Following up on this work, we set out to examine whether *MLL*-r cell line models could acquire pinometostat resistance through continuous treatment at concentrations above the predetermined 14-day proliferation assay IC_{90} (37). Resistance to pinometostat in all five cell lines tested emerged following 3 weeks of continued treatment and was defined by increased growth rates in the presence of inhibitor. In depth analysis of two *MLL*-r models KOPN-8 (*MLL-ENL*) and NOMO-1 (*MLL-AF9*) identified common characteristics between the resistant cell lines, but distinct mechanisms by which they became resistant. These mechanisms included examples of increased expression of drug efflux transporters and evidence of activation of signaling pathways such as PI3K/AKT and RAS/RAF/MEK/ERK.

Materials and Methods

Cell culture and analysis of cell proliferation and viability

Human leukemia cell lines KOPN-8 (ACC 552), NOMO-1 (ACC 542), MOLM-13 (ACC 554), and SEM (ACC 546) were obtained from DSMZ, whereas MV4-11 (CRL-9591) cells were attained from ATCC, between the years 2009 to 2010. All cell lines were authenticated by STR profiling (KOPN-8 and NOMO-1 cells were authenticated using the ATCC fee for service; MOLM-13, MV4-11, and SEM were authenticated by the vendors and used within 6 months of resuscitation), and grown in vendor recommended media (all cell culture reagents were supplied by Thermo Fisher Scientific) in a humidified incubator set to 37°C and 5% CO_2. Pinometostat-resistant cells were cultured in media supplemented with 1 μmol/L (MV4-11, MOLM-13) or 4.5 μmol/L (KOPN-8, NOMO-1, SEM) of the inhibitor. Every 3 to 4 days, cell number and viability was assessed by Trypan blue exclusion staining (Vi-CELL, Beckman Coulter) and growth media and pinometostat replaced, splitting cells back to a density of 2×10^5 cells/mL. Cell splitting ratios were recorded and used to express the total number of viable cells per milliliter. Pinometostat was made by Epizyme (38). Proliferation assays with combination agents valspodar (PSC 833, R&D Systems), trametinib (Selleck Chem), GDC-0994 (Selleck Chem), and dabrafenib (Selleck Chem) were completed with the above conditions (39–42).

ELISA analysis on inhibition of H3K79me2

The H3K79me2 ELISA was performed as previously described (25). Briefly, 1 to 2×10^6 KOPN-8 and NOMO-1 cells were collected after 10 and 28 days of dosing with 4.5 μmol/L pinometostat or DMSO. Histones were extracted as previously described (21). Histones were run in matched H3K79me2 and total H3 ELISAs. The optical density of the H3K79me2 ELISA was normalized to the total H3 ELISA of each sample.

Sanger sequencing

Cell pellets from the resistant and parental KOPN-8 and NOMO-1 cell lines were provided to Genewiz for endogenous cDNA verification of DOT1L by Sanger sequencing. RNA extraction and purification was performed with the RNeasy Plus Mini Kit (Qiagen, 74134) followed by cDNA library generation with the SuperScript III First-Strand Synthesis Supermix Kit (Invitrogen, 18080-400). A 1% agarose gel was used to resolve PCR products, followed by purification with the Qiaquick Gel Extraction Kit (Qiagen, 28706). The procedures followed for the RNA extraction, cDNA library generation, and gel extraction were completed as outlined in the manufacturer's protocols. BigDye Terminator Cycle Sequencing was used for sequencing and DNASTAR Lasergene12 software for data analysis. The threshold for SNP detection was set to 10%. Sequencing results were compared to the reference sequence NM_032482.2. PCR and sequencing primers can be found in the Supplementary Methods. *DOT1L* sequences were deposited in GenBank for KOPN-8 (accession number KX792913) and NOMO-1 (accession number KX792914).

Quantitative real-time PCR

Total RNA was isolated from approximately 3×10^6 cells using the RNeasy Total RNA Isolation Kit (Qiagen, 74106) according to manufacturer's instructions. *ABCB1* (Hs00184500_m1, Thermo Fisher Scientific) mRNA levels were assessed and normalized to *18S* (Hs99999901_s1, Thermo Fisher Scientific), *HOXA9* (Hs00365956_m1, Thermo Fisher Scientific), and *MEIS1* (Hs00180020_m1, Thermo Fisher Scientific) were assessed and normalized to beta-2-microglobulin (*B2M)* (4333766F, ThermoFisher Scientific) by qRT-PCR as previously described (21).

RNA-seq

Samples were collected after 28 days (KOPN-8) or 53 days (NOMO-1) of 4.5 μmol/L pinometostat treatment for whole transcriptome analysis through RNA-seq. To distinguish changes in gene expression due to DOT1L inhibition from acquired resistance, naïve cells were dosed with 4.5 μmol/L pinometostat for 10 days and included in the RNA sequencing analysis as a reference for sensitivity to pinometostat. All samples were then evaluated relative to the vehicle control. Q^2 Solutions performed the RNA extraction, amplification, and microarray processing on the samples detailed above. RNA-seq data was deposited in GEO, accession number GSE94849.

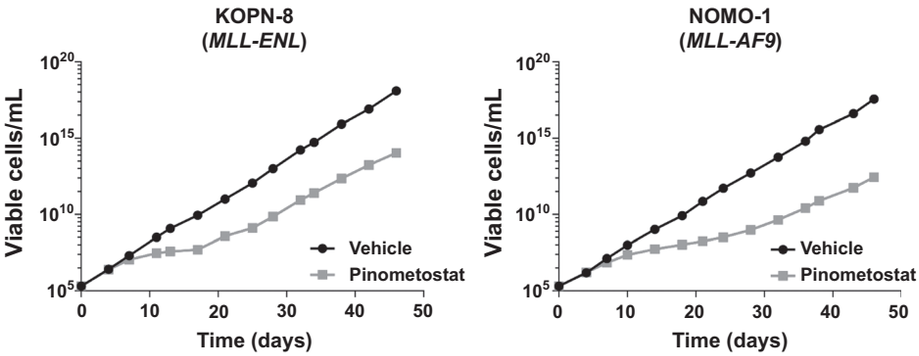

Figure 1.

Development of pinometostat resistance in cell line models of *MLL*-r. Cellular *MLL*-r models sensitive to single-agent treatment of pinometostat were continuously treated with 4.5 μmol/L inhibitor to determine if resistance would develop. The cell lines KOPN-8 and NOMO-1 regained growth rates similar to the vehicle control after approximately 21 days of dosing. Following the transition to a pinometostat refractive state, both cell lines were maintained in growth media containing pinometostat to assure the resistant pool was stable. Viable cells were counted and split every 3 to 4 days in the presence of pinometostat or DMSO vehicle control and split adjusted results plotted on a logarithmic scale.

Detailed library preparation and sequencing methods can be found in the Supplementary Methods.

H3K79me2 chromatin immunoprecipitation followed by sequencing

Samples were collected from KOPN-8 cells treated with 4.5 μmol/L pinometostat or DMSO for 10 and 28 days, and from NOMO-1 cells treated for 14 and 53 days. Cells were fixed for chromatin immunoprecipitation followed by sequencing (ChIP-seq) according to the protocol provided by Active Motif as follows. 1/10 volume of formaldehyde solution (11% formaldehyde, 0.1 mol/L NaCl, 1 mmol/L EDTA, pH 8, 50 mmol/L HEPES pH 7.9) was added to the media of each flask of cells. Following agitation at room temperature for 15 minutes, fixation was halted with the addition of 1/20 volume 2.5 M glycine solution for 5 minutes. Cells were spun down in a 4°C cooled microcentrifuge at 800 × *g* for 10 minutes and the supernatant removed. Following centrifugation, cells were washed with 10 mL ice cold PBS-Igepal (1× PBS, 0.5% Igepal CA-630) and supernatant removed. Cells were washed again with 10 mL ice cold PBS-Igepal with the addition of 100 μL PMSF (100 mmol/L in ethanol, final concentration 1 mmol/L). Cell pellets were flash frozen and stored at −80°C.

Fixed samples were provided to Active Motif for chromatin immunoprecipitation with an antibody against H3K79me2 (Abcam, ab3594) and next-generation sequencing. Detailed methods can be found in the Supplementary Methods.

ABCB1 transporter study

ABCB1 transporter studies were performed at Optivia Biotechnology as described in the Supplementary Methods.

Western blot analysis

For details, please see Supplementary Methods.

Bioinformatics analysis

Utilizing different R packages, PCA, hierarchical clustering, differentiation, and pathway analyses were performed on the RNA-seq data as described in the Supplementary Methods.

Results

Development of pinometostat resistance in KOPN-8 and NOMO-1 cell line models of *MLL*-r

MLL-r cell lines KOPN-8 (*MLL-ENL*) and NOMO-1 (*MLL-AF9*) are examples of cellular models that have demonstrated antiproliferative phenotypes, with 14 day IC_{50} values of 71 and 658 nmol/L respectively, when treated with pinometostat as a single agent (25). We tested the potential for identifying resistance mechanisms using these two sensitive *MLL*-r models by treating each cell line continuously in the presence of 4.5 μmol/L pinometostat until resistance was acquired. The process to achieve pinometostat resistance for both cell lines was completed within approximately 3 weeks from the initiation of treatment (Fig. 1). We have previously demonstrated approximately 7 days of treatment with pinometostat is required to realize clear antiproliferative activity *in vitro* (25). Antiproliferative activity in the form of cell stasis continues from day 7 through day 20, after which a resistant phenotype emerges. Resistance was defined as when the growth rate of the cells cultured in the presence of pinometostat was similar to the naïve control cell line. Stability of the resistant cell line pools was ascertained by allowing the cells to grow in the presence of pinometostat for an additional 3 weeks following the establishment of resistance.

Table 1. Inhibition of H3K79 methylation and cellular proliferation by pinometostat in control and resistant cell lines

Parameter[a]	Cell type		Fold-change[b]
	KOPN-8		
	Control	Resistant	
H3K79me2 IC_{50} (μmol/L)	0.015 ± 0.016	2.32 ± 0.35	154
Antiproliferative IC_{50} (μmol/L)	0.041 ± 0.060	29.21 ± 40.75	711
	NOMO-1		
	Control	Resistant	
H3K79me2 IC_{50} (μmol/L)	0.027 ± 0.025	0.095 ± 0.004	3
Antiproliferative IC_{50} (μmol/L)	0.111 ± 0.021	>50	>449

Pinometostat 4 day H3K79me2 IC_{50} (μmol/L) and 14-day long-term proliferation IC_{50} (μmol/L) measured in the control and resistant cell lines.

[a]± error represents the 95% confidence interval.

[b]Fold-change calculated as [(resistant − control)/control] values.

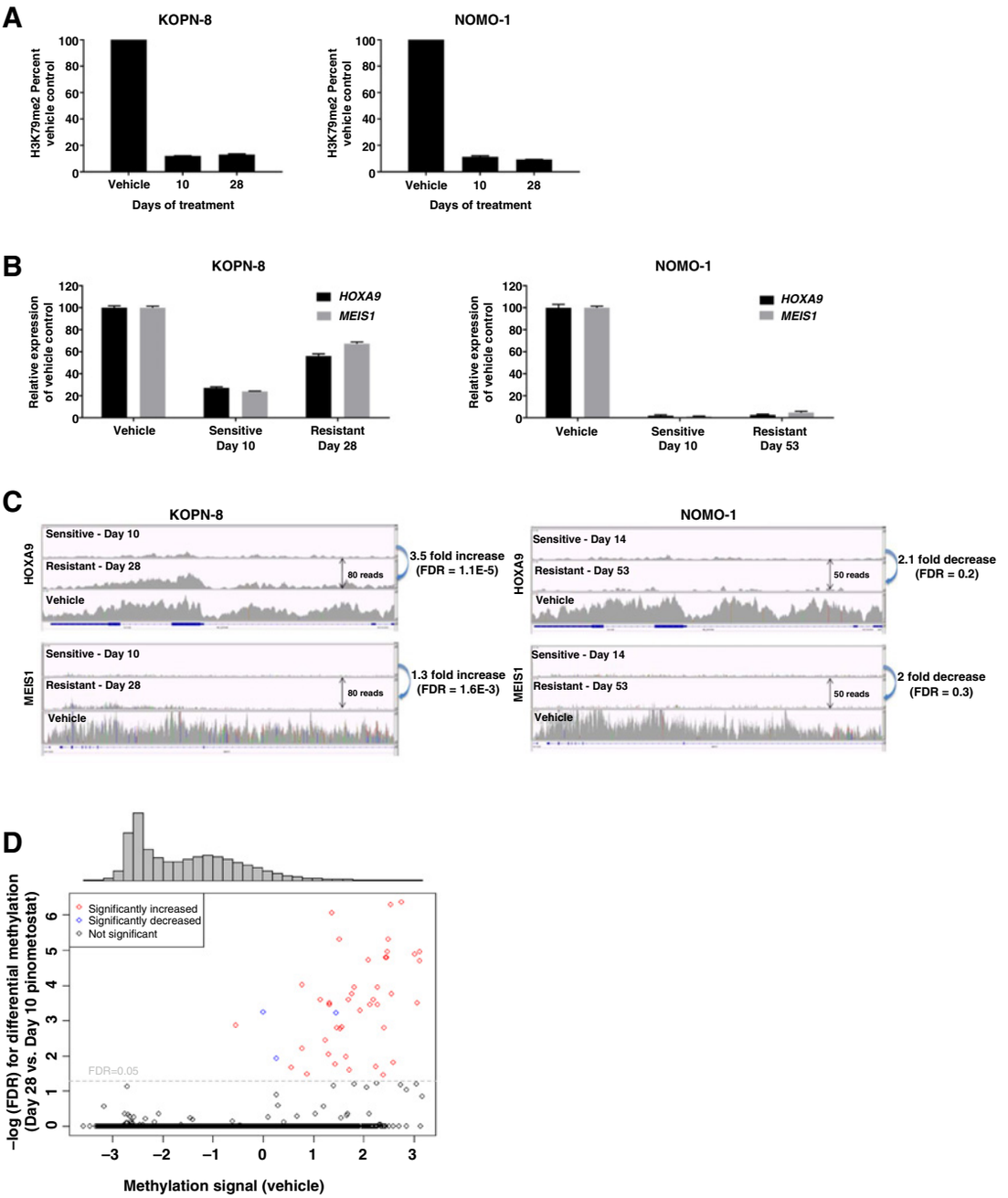

Figure 2.

Measures of pharmacodynamic markers over time. Analysis of pharmacodynamic markers over the course of development of resistance. **A,** Global H3K79me2 analysis by ELISA in KOPN-8 and NOMO-1 cells following treatment with 4.5 μmol/L pinometostat at indicated time points. H3K79me2 levels are plotted as a percentage of vehicle control. **B,** RNA-seq analysis of DOT1L target genes in KOPN-8 and NOMO-1 vehicle control, pinometostat sensitive and pinometostat-resistant cells. Relative mRNA expression levels are plotted as a percentage of those in vehicle-treated control cells. *HOXA9* and *MEIS1* gene expression begins to recover in resistant KOPN-8 cells, while no recovery of target gene expression is observed in resistant NOMO-1 cells. **C,** Assessment of H3K79me2 at *HOXA9* and *MEIS1* gene loci using ChIP-seq. The difference between the sensitive and resistant cell lines is shown as the FDR corrected *P*-value (*q*-value). Significant recovery ($q \leq 0.05$) of H3K79me2 was observed at both the *HOXA9* and *MEIS1* gene loci as the KOPN-8 cells developed resistance to pinometostat. No significant recovery of H3K79me2 was observed in NOMO-1 cells at any locus. **D,** KOPN-8 ChIP-seq data plotted as the significance [−log(FDR)] of the change in H3K79me2 methylation levels between the day 28 vs. day 10 treatment vs. the baseline methylation status. The majority of the significant changes in methylation status ($q \leq 0.05$) occurs in genes with high baseline methylation signal. The histogram above the plot demonstrates the distribution of genes across the methylation signal spectrum. Genes with a high baseline methylation signal represent only a small portion of all genes assessed.

Cellular responses to pinometostat in resistant and control pools were examined by a number of pharmacological measures (Table 1) including proliferation rates and the ability to inhibit the DOT1L pharmacodynamic marker H3K79me2. In both the KOPN-8 and NOMO-1 cells tested, there was a hundreds-fold increase in proliferation IC_{50} values between the control and resistant cell lines. Interestingly, despite similar shifts in proliferation IC_{50} values, the degree of H3K79me2 inhibition four days posttreatment was discordant between the KOPN-8- and NOMO-1–resistant cells. In KOPN-8 cells, much like the proliferation shift, there was an approximate 100-fold increase in IC_{50} values for inhibition of the H3K79me2 mark between the control and resistant cell lines, from 15 to 2 μmol/L, suggesting a significant decrease in target inhibition. In contrast, the NOMO-1 cell lines exhibited a muted shift of a less than three-fold increase in the H3K79me2 mark IC_{50} values between the control and resistant cell lines, from 27 to 95 nmol/L. The rate at which both of these cell lines became refractory to pinometostat is suggestive of the acquisition of a mutation in the SAM binding domain of DOT1L or increased activity of a drug efflux transporter. The pharmacologic measurements in Table 1 potentially support either hypothesis as the mechanism for KOPN-8 resistance, as the shift in cell growth inhibition and H3K79me2 is suggestive of the drug's decreased ability to interact with DOT1L. The sustained inhibition of H3K79me2 in pinometostat-resistant NOMO-1 cells is in contrast to the KOPN-8 results and could indicate alternative mechanisms of pinometostat resistance.

Measures of pharmacodynamic markers over time

To further evaluate the mechanistic differences between pinometostat resistance in the KOPN-8 and NOMO-1 cells, we collected cells at various time points over the course of developing pinometostat resistance. Samples from these time points underwent detailed analyses of global and locus specific H3K79me2 in addition to whole transcriptome analysis through RNA-seq. Assessment of global H3K79me2 from resistant samples continuously maintained in 4.5 μmol/L pinometostat, a dose higher than the IC_{50} for global reduction of H3K79me2, demonstrated that relative to their DMSO (vehicle) controls, both the resistant KOPN-8 and NOMO-1 cells exhibited maximal and sustained inhibition of the H3K79me2 mark across both time points evaluated, at approximately 10% of the vehicle control (Fig. 2A). RNA-seq analysis was performed in an attempt to identify signaling pathways altered by the development of pinometostat TER. Using these data to assess *MLL*-r target genes *HOXA9* and *MEIS1* in the KOPN-8 and NOMO-1–resistant cell lines, we noted a divergence in response between the two cell lines (Fig. 2B). The effects of DOT1L inhibition through either small molecule inhibition or genetic knockdown have established that loss of DOT1L enzymatic activity will lead to decreased transcription of *MLL*-r target genes *HOXA9* and *MEIS1* (11, 16, 21, 25). As shown in Figure 2B, resistant KOPN-8 cells maintained significantly higher levels of *HOXA9* and *MEIS1* in the presence of pinometostat than their sensitive counterparts. In contrast, both resistant and sensitive NOMO-1 cells showed similar depletion of *HOXA9* and *MEIS1*, suggesting that two different resistance mechanisms may be at work. Moreover, these data also suggest that KOPN-8 cells are able to maintain *HOXA9* and *MEIS1* levels even when global H3K79me2 is reduced. To understand the discrepancy between the persistent global inhibition of H3K79me2 and recovery of target gene expression in the resistant KOPN-8 cells, we performed ChIP-seq using an antibody specific for the dimethylation state of H3K79 (Fig. 2C). Results from the ChIP-seq provided a potential explanation for how target gene expression recovered in the KOPN-8–resistant cells, despite sustained global methyl mark inhibition. In the sensitive KOPN-8 cells, reduced methylation was observed across the entire genome while the resistant cells showed significantly increased methylation at many *MLL*-r target gene loci, including *HOXA9* and *MEIS1*. Thus, despite global methylation inhibition in the resistant KOPN-8 line, we propose that the recovery of H3K79me2 levels at key target genes reactivated transcription, as observed with *HOXA9* and *MEIS1*. An evaluation of all genes with recovered H3K79me2 in the resistance setting reveals a significant overlap with genes harboring high baseline H3K79me2 (Fig. 2D). Unlike the KOPN-8 line, gene specific H3K79me2 inhibition was maintained across the whole genome in both the resistant and sensitive NOMO-1 cells.

Overexpression of drug efflux transporter ABCB1 correlates with primary and secondary resistance to pinometostat

Increased expression and function of drug transporters is a common mechanism for both primary and secondary resistance to anticancer drugs (43–46). Drug metabolism studies performed with pinometostat identified it as a substrate for the common drug transporter ATP-binding cassette subfamily B member 1 (ABCB1, P-gp, P-glycoprotein, MDR1; Supplementary Table S1). Based on this result, we reviewed our RNA-seq data to determine if development of pinometostat resistance influenced the expression of a

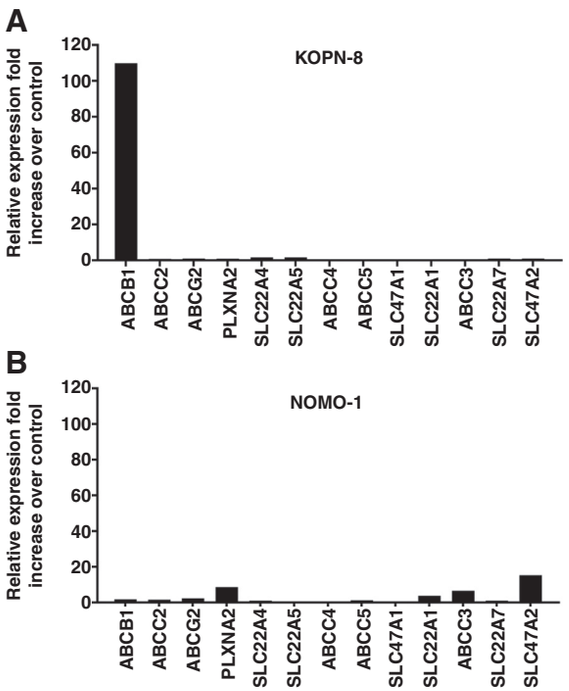

Figure 3.

Membrane transporter mRNA expression in resistant cell lines. RNA-seq analysis of common drug efflux transporters in (**A**) KOPN-8–resistant cells at day 28 of treatment and (**B**) NOMO-1–resistant cells at day 53 of treatment, plotted as the fold change in RNA-seq counts in the resistant versus control cell line.

set of membrane transporters commonly assessed in small molecule drug development. Examination of expression data from this panel of transporters revealed that resistant KOPN-8 cells had a greater than 100-fold increase in *ABCB1* expression over the vehicle control cells (Fig. 3A). In contrast, and consistent with sustained *HOXA9* and *MEIS1* inhibition, little to no change in *ABCB1* expression was observed in the resistant NOMO-1 cell line (Fig. 3B). Based on these data it is reasonable to suspect activity of a drug efflux transporter is responsible for the recovery of H3K79me2 and *MLL*-r target genes in our KOPN-8 pinometostat-resistant cell line model.

Expression of *ABCB1* has been described as a poor prognostic factor for elderly patients with AML and has been implicated with relapsed AML, leukemia arising from myelodysplastic syndrome, and treatment with certain anticancer therapies such as daunorubicin (47–49). We sought to determine if a correlation existed between *ABCB1* expression and the inhibitory effect of pinometostat on H3K79me2 levels. We measured *ABCB1* expression levels by qPCR in a panel of leukemia cell lines and observed a wide range of expression, from undetectable to up to nearly 250 times the expression of the lowest detectable expression (Fig. 4A and Supplementary Table S2). We then determined the H3K79me2 IC_{50} after 4-day treatment with pinometostat in a subset of the leukemia cell lines. In the cell lines with detectable expression of *ABCB1*, the relative expression of *ABCB1* correlated with the H3K79me2 IC_{50} for that line (Fig. 4B). Of the cell lines analyzed, the non-*MLL*-r AML line KG-1a had the highest expression of *ABCB1* and correspondingly greatest H3K79me2 IC_{50}. To determine if high *ABCB1* expression was causing the high H3K79me2 IC_{50} in the KG-1a cell line, we cotreated KG-1a with pinometostat and the ABCB1 inhibitor, valspodar (PSC-833; Fig. 4C). Valspodar is a non-immune suppressant analogue of cyclosporin A and has been tested clinically in combination with a variety of anticancer treatments, including paclitaxel, doxorubicin, and daunorubicin (50–54). When the KG-1a cell line was treated with pinometostat and valspodar, the H3K79me2 IC_{50} was significantly reduced.

Discovering that inhibition of ABCB1 led to increased target engagement in a model with inherent overexpression, we sought to confirm the extent to which the mechanism of resistance in the KOPN-8–resistant cells was mediated by overexpression of ABCB1. We dosed both the resistant KOPN-8 and NOMO-1 cell lines with a combination of pinometostat and valspodar (Fig. 5A). Inhibition of ABCB1 through valspodar fully resensitized the resistant KOPN-8 cells to the action of

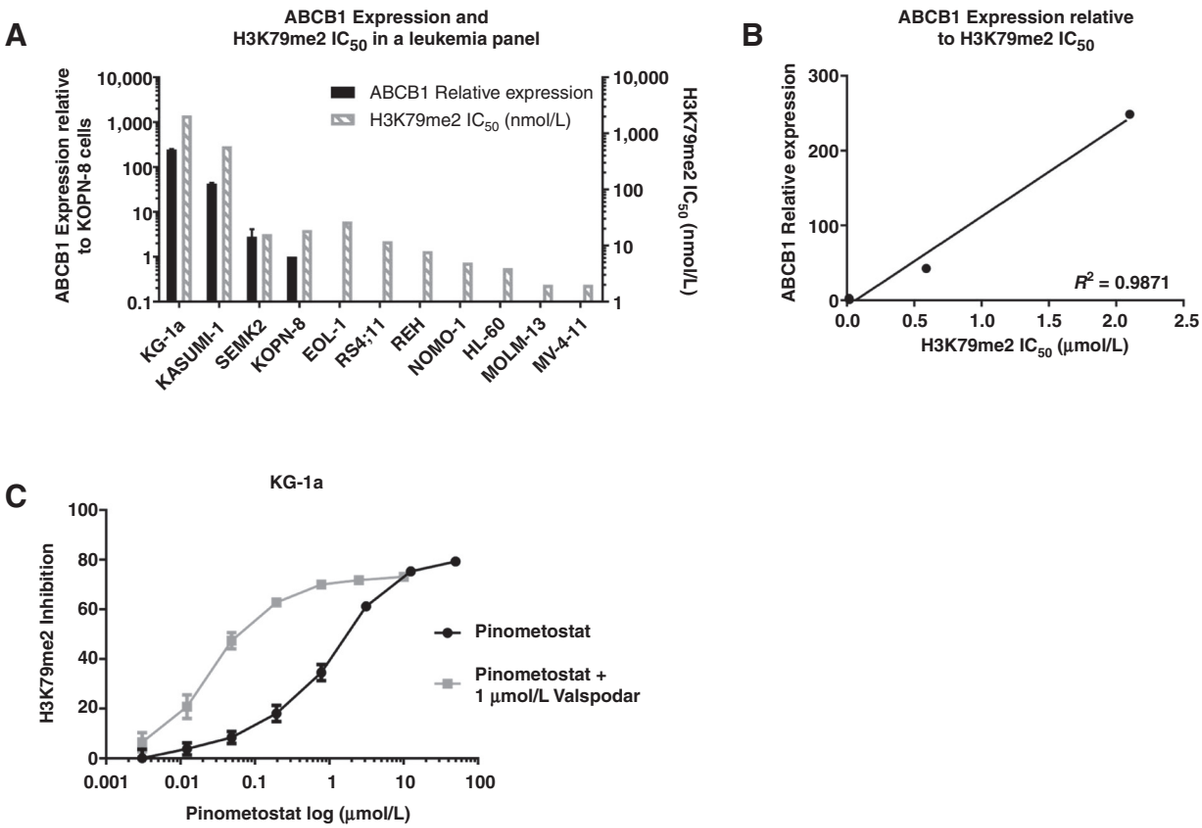

Figure 4.

Overexpression of *ABCB1* positively correlates with primary resistance to pinometostat. Correlation of *ABCB1* expression with primary resistance to pinometostat in a panel of leukemia cell lines. (**A**) Quantitative real-time PCR analysis of *ABCB1* expression and H3K79me2 IC_{50} values in a panel of leukemia cell lines. Relative mRNA expression levels are plotted relative to KOPN-8. Table of H3K79me2 IC_{50} values available in Supplementary Table S2. (**B**) Correlation of *ABCB1* expression with H3K79me2 IC_{50} values. (**C**) *ABCB1*-high cell line KG-1a was treated with pinometostat single agent or in combination with 1 μmol/L valspodar for 4 days, and inhibition of H3K79me2 mark assessed by ELISA.

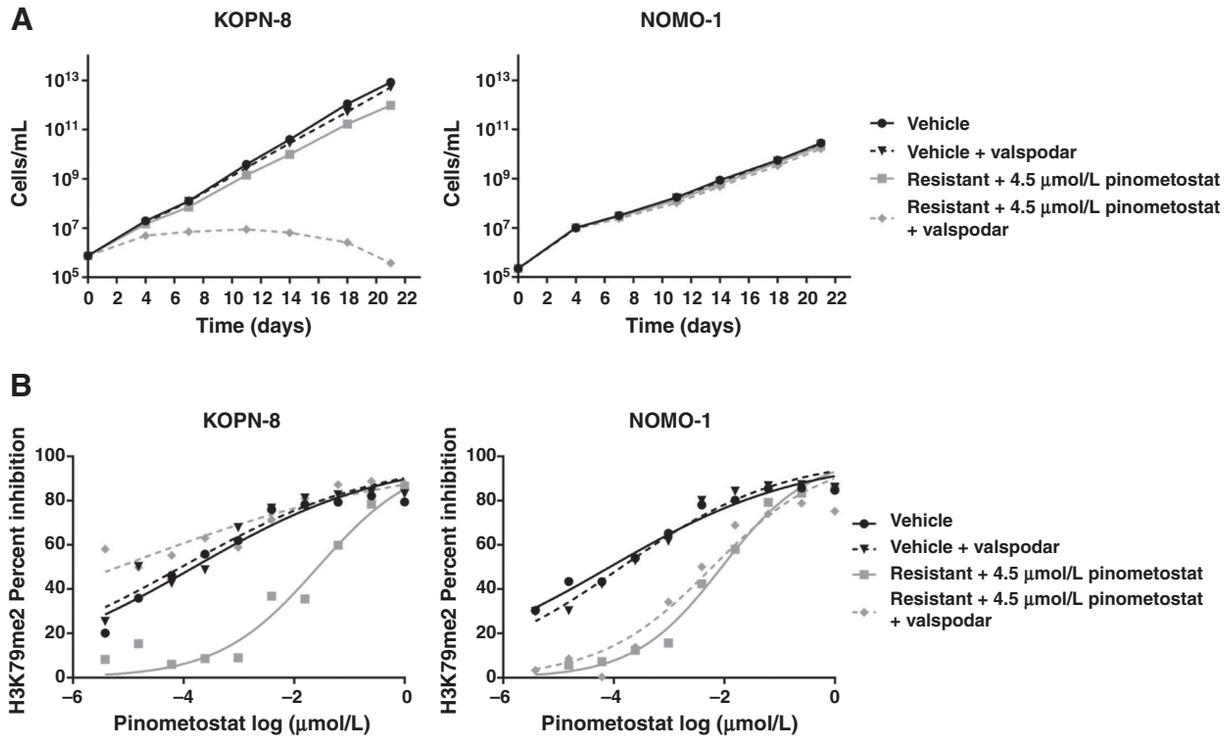

Figure 5.

Pinometostat resensitization of KOPN-8 but not NOMO-1–resistant cell lines achieved through dosing in combination with valspodar. Resensitization of ABCB1-mediated resistance with ABCB1 inhibitor. **A,** Growth of KOPN-8 and NOMO-1–resistant and DMSO vehicle control cells when treated with 1 μmol/L valspodar for 21 days. Resistant cells were cultured in media containing 4.5 μmol/L pinometostat. Viable cells were counted and split every 3 to 4 days and split adjusted results plotted on a logarithmic scale. **B,** Global H3K79me2 analysis by ELISA in resistant KOPN-8 and resistant NOMO-1 cells following combination treatment with 1 μmol/L valspodar and pinometostat at indicated concentrations for 4 days. H3K79me2 levels are plotted as a percentage of vehicle control.

pinometostat, as evidenced by their reduced growth rate from day 4 through the end of the experiment at day 21. No effects on growth were observed in the KOPN-8 control line with single-agent valspodar (Fig. 5A). After 4 days of cotreatment with valspodar in the KOPN-8 and NOMO-1 cell lines, we also assessed H3K79me2 at several concentrations (Fig. 5B). Treating the resistant KOPN-8 cells with valspodar and pinometostat shifted H3K79me2 back to a similar level as the naïve cells treated with pinometostat alone. To verify drug transporters were not playing a role in the NOMO-1 resistance, we also dosed these cells in combination with valspodar and pinometostat. Valspodar had no single agent activity with the NOMO-1 cells, nor did it resensitize the resistant cells to pinometostat, consistent with an ABCB1 independent mechanism of pinometostat resistance in NOMO-1 (Fig. 5A). Samples were also collected for analysis of H3K79me2 and the results were consistent with the proliferation results, as the combination with valspodar had no effect (Fig. 5B).

Additional *MLL*-r models support overexpression of ABCB1 as the primary TER mechanism

Because our studies identified two distinct resistance mechanisms we wanted to test additional *MLL*-r models to identify if there was a common mechanism among *MLL*-r cell lines. Additional *MLL*-r cell lines, MV4-11 (*MLL-AF4*), MOLM-13 (*MLL-AF9*), and SEM (*MLL-AF4*) were treated continuously with pinometostat, and similar to the KOPN-8 and NOMO-1 cells, acquired resistance within 3 weeks from the initiation of treatment. All three of these additional models demonstrated that the phenomenon of *ABCB1* overexpression was not unique to the KOPN-8 cells, with fold increases of *ABCB1* ranging from 10 to 2,000 times the vehicle control (Supplementary Fig. S1A). We then sought to determine if the mechanism of resistance was mediated by overexpression of ABCB1. Utilizing the MV4-11- and SEM-resistant cell lines, we treated with a combination of pinometostat and valspodar. Inhibition of ABCB1 with valspodar fully resensitized both the MV4-11 and SEM cell lines to the effect of pinometostat (Supplementary Fig. S1B). Results from these additional cell lines identify *ABCB1* overexpression as a common mechanism by which *MLL*-r cell lines can bypass the effect of pinometostat.

Hypothesis generation and testing of NOMO-1 mechanism of resistance

With the inability of valspodar to resensitize NOMO-1 cells to pinometostat treatment and minimal increase in *ABCB1* expression observed in these cells, we set out to determine what other mechanisms were playing a role in the NOMO-1 resistance. Published results with another PMT, EZH2, demonstrated that one potential mechanism of resistance in this enzyme family is through acquisition of a secondary mutation leading to decreased binding of small molecule inhibitors (35, 36). To explore if

NOMO-1 cells acquired resistance through a secondary mutation, DNA was obtained from both the parental and TER NOMO-1 cells and subjected to Sanger sequencing across the full coding region of *DOT1L*. In addition to sequencing the NOMO-1 cells, we also obtained DNA from KOPN-8 parental and TER cells, as a representative model from the group demonstrating ABCB1 overexpression as the primary mechanism of resistance. In both cell line models the *DOT1L* sequence remained unchanged between parental and resistant lines. Therefore, we were unable to detect any evidence of a resistance mechanism for pinometostat being driven through the acquisition of mutations within *DOT1L* (Supplementary Fig. S2). Given the apparent lack of pinometostat-selected mutations in *DOT1L*, we investigated possible alternative mechanisms which could potentially lead to pinometostat resistance.

Detailed gene expression and pathway analysis was performed on the ChIP-seq and RNA-seq data sets generated from the naïve and resistant NOMO-1 cell lines. Principal component analysis of the RNA-seq data demonstrated that NOMO-1 cell line gene expression signatures could be distinguished by whether they were treated with pinometostat or vehicle (PC1) and their pinometostat sensitivity status and treatment time, that is, resistant or naïve cell line status (PC2), indicating that altered gene expression occurs following pinometostat exposure and likely plays a role in the development of resistance (Supplementary Fig. S3). Combined analysis of the ChIP-seq and RNA-seq data identified many potential mechanisms involved in the development of resistance, including the PI3K/AKT and RAS/RAF/MEK/ERK signaling pathways, the latter being of greater interest to us due to the availability of a number of specific inhibitors targeting a variety of nodes in the pathway (Supplementary Fig. S4A–S4C, Supplementary Tables S3 and S4; ref. 55). We tested combinations of pinometostat with MEK, ERK, and BRAF inhibitors in the resistant NOMO-1 cells. We first determined IC_{50} values in naïve NOMO-1 cells then used those doses to treat in combination to determine whether the inhibitors could resensitize the resistant NOMO-1 cells. None of the three compounds tested (trametinib, GDC-0994, and dabrafenib) were effective in resensitizing the resistant NOMO-1 cells to pinometostat (Supplementary Fig. S5; refs. 40, 41). Of note, both the control and resistant NOMO-1 lines displayed exquisite single agent sensitivity to the MEK1/2 inhibitor trametinib with 3-day IC_{50} values less than 1 nmol/L (40). To reconcile the lack of resensitization of the resistant NOMO-1 line with inhibitors of the RAS/RAF/MEK/ERK signaling pathway with the finding of pathway activation, we measured levels of phospho-proteins in the RAS/RAF/MEK/ERK pathway by immunoblot. Consistent with the proliferation results, we did not observe any changes in levels of protein phosphorylation between the control and resistant NOMO-1 lines (Supplementary Fig. S6). The lack of pathway activation as determined by phospho-protein suggests that although the gene expression data indicated key pathway signaling in the resistant cell lines, this change in transcription did not appear to translate functionally into altered pathway activation as measured by phosphorylation status of the pathway components. Thus, although RAS/RAF/MEK/ERK signaling may be altered transcriptionally in the resistant NOMO-1 cell line, this alteration does not appear to be driving resistance to pinometostat. To further interrogate the RNA-seq data set, pathway analysis was performed using the KEGG, GO—Biological Process, and MSigDB databases comparing the resistant cell line with the pinometostat treated (sensitive) parental cell line. From the KEGG and GO analysis, 838 and 313 significant pathways were identified, respectively. In the MSigDB analysis, of 1,036 gene sets, none were significantly (FDR < 0.05) upregulated whereas 26 were significantly downregulated (Supplementary Tables S5 and S6). The most highly significant pathways were largely unrelated to established oncogenic pathways, but these results provide future avenues for potential investigation into the molecular understanding of NOMO-1 TER.

Discussion

DOT1L is known to play a role in *MLL*-r leukemia through its recruitment by MLL fusion proteins and subsequent hypermethylation of a characteristic set of genes known to drive leukemogenesis (9, 10, 16). The strong scientific rationale supporting the role of DOT1L in a subtype of acute leukemias makes it a target of interest for cancer treatment. With clinical development of pinometostat ongoing we sought to identify potential mechanisms leading to TER.

Small molecule based targeted therapies have greatly expanded the options available for oncology patients, and resistance to those drugs can emerge. A common resistance mechanism found with many of the tyrosine kinase inhibitors is the acquisition of molecular variants ranging from single nucleotide changes to intragenic deletions (27). Specifically in the PMT family, which includes DOT1L and EZH2, publications by Gibaja and colleagues and Baker and colleagues highlighted secondary mutations in both wild-type and mutant *EZH2* alleles leading to resistance of specific small molecule PMT inhibitors in preclinical *in vitro* models (35, 36). In this study, we developed five *MLL*-r cell line models of acquired pinometostat resistance. Sanger sequencing of *DOT1L* in the KOPN-8 and NOMO-1 cell lines determined that our resistant pools had not acquired a secondary mutation. However, given the limitations of Sanger sequencing for detecting low variant allelic frequencies we cannot exclude the possibility of the existence of a subclonal *DOT1L* mutation. Given that the subclone would not likely be a driver of resistance, we believe we uncovered PMT resistance mechanisms beyond what was previously described in the literature.

The observation that marginal recovery of H3K79me2 at specific *MLL*-r target loci led to reactivation of *HOXA9* and *MEIS1* transcription strongly suggests a threshold increase in H3K79me2 levels is required to support a resistant state. However, once this threshold is reached, the loss of H3K79me2 at remaining genetic loci does not impact the cell's viability or typical functionality. A well-known mechanism of drug resistance is the overexpression of drug efflux transporters (43–46). We mined our RNA-seq data comparing naïve and resistant pools looking specifically at transcripts of transporters highlighted by the FDA as being clinically significant to drug–drug interactions (56). Several transporters published in the FDA guidance also play a role in drug resistance such as ABCB1 and ABCG2 (57). Analysis of the RNA-seq data identified greater than 100-fold upregulation of *ABCB1* in KOPN-8–resistant cells. Overexpression of ABCB1 is consistent with the focused recovery of H3K79me2 at genes critical to driving proliferation and maintaining a cell differentiation block. Following this observation, we treated resistant KOPN-8 cells with an inhibitor of ABCB1 and were able to resensitize the cells to pinometostat. These results suggest the mechanism of resistance is likely due to decreased intracellular levels of pinometostat in KOPN-8–resistant cells, due to rapid efflux via the ABCB1

transporter. Considering inhibition of ABCB1 is not currently a viable clinical strategy, the question remains as to how this mechanism of resistance might be handled clinically. One potential strategy would be to develop a new generation of DOT1L inhibitors with a drug design emphasis on removing characteristics which lead to the molecule being a substrate for drug efflux. Lead candidates from a new series of inhibitors could be screened in models of resistance and/or cellular biochemical assays run in cell lines that have high baseline expression of ABCB1 such as KG-1a. Alternatively, signaling pathways responsible for the modulation of ABCB1 expression could also be investigated. However, these signaling pathways are known to be complex and varied and to date have yet to be validated as a clinically relevant mechanism of pinometostat resistance (45, 46).

The NOMO-1 cell line generated with resistance to pinometostat was established to have a mechanism distinct from drug efflux. This observation led us to explore pathways identified through transcript analysis as being altered between the naïve and resistant cells. Unlike ABCB1, several of the pathways identified in the resistant NOMO-1 cells are druggable with clinically relevant inhibitors and could easily be tested to determine if pathway inhibition resensitized the cells to pinometostat. Treatment of resistant NOMO-1 cells with representative inhibitors of the RAS/RAF/MEK/ERK signaling pathway (e.g. dabrafinib and trametinib) failed to resensitize the cells to pinometostat. These data suggest that mechanisms and pathways identified through our analysis of transcripts did not represent cellular dependence on increased signal transduction of this pathway. Indeed, when we probed protein lysates harvested from naïve and resistant NOMO-1 cells we saw no evidence of increased phosphorylation of the RAS/RAK/MEK/ERK pathway. Although not all pathways shown to be differentially expressed by RNA-seq were exhaustively pursued, we believe that given the lack of active signaling, further exploration would have a low probability of success. AML is a complex disease with multiple molecular variants capable of driving leukemogenesis (58–60). Considering NOMO-1 cells harbor a *KRAS* G13D mutation, it is possible that *MLL*-r may not be the main oncogenic driver (61). Unsurprisingly, NOMO-1 cells were exquisitely sensitive to single-agent treatment with the MEK inhibitor trametinib. Given the timeframe to development of pinometostat resistance, along with the maintenance of H3K79me2 inhibition both globally and at *MLL*-r target gene loci, it is conceivable that the development of resistance indicated a shift from reliance on programming caused by the *MLL–AF9* fusion to RAS pathway addiction.

Although our investigations in this manuscript utilized established cell line models, the authors believe corroboration of pinometostat resistance in primary patient samples would provide more clinical relevance. However, these studies cannot currently be performed given the limited life span of primary patient samples and the extended timeframe required to induce resistance. Furthermore, the potential for investigation of TER *in vivo* is limited by the pharmacokinetic properties and exposure levels of pinometostat needed to perform xenograft studies, necessitating delivery through a continuous intravenous infusion in nude rats. Delivery of pinometostat through continuous intravenous infusion presents additional challenges due to the extended dosing period required and the need to maintain pump and IV line integrity for several weeks. Given the practical limitations of alternative models and the need for long-term maintenance of pinometostat exposure to drive resistance, apart from a clinical trial, cell lines are currently the only human model system in which it is feasible to explore pinometostat resistance.

In summary, we developed several novel models of resistance to the DOT1L inhibitor pinometostat. The evidence provided suggests that resistance was not induced via a direct target mutation-based mechanism. Instead, investigations into the mechanisms of TER identified that two independent mechanisms were operating in our cell line models. In four of the five resistant models we observed a clear association of pinometostat activity with *ABCB1* overexpression, and *ABCB1* was identified as the likely primary mechanism of acquired pinometostat resistance. In contrast the NOMO-1 mechanism of resistance remains unknown but is independent of ABCB1. Development of these cell line models and understanding the mechanisms of resistance may have utility in exploring clinical mechanisms of resistance to pinometostat.

Disclosure of Potential Conflicts of Interest

C.T. Campbell is a principal research associate at Epizyme and has ownership interest (including patents) in Epizyme. R.M. Pollock has ownership interest (including patents) in Epizyme. J.J. Smith has ownership interest (including patents) in Epizyme stock options. R.A. Copeland has ownership interest (including patents) in Epizyme, Mersana, and Raze Therapeutics; and is a consultant/advisory member for Mersana, Raze Therapeutics, and Synergy Partners. No potential conflicts of interest were disclosed by the other authors.

Authors' Contributions

Conception and design: C.T. Campbell, N.J. Waters, E.J. Olhava, R.M. Pollock, J.J. Smith, R.A. Copeland, S.J. Blakemore, K.M. Bernt, S.R. Daigle

Development of methodology: C.T. Campbell, N.J. Waters, S.J. Blakemore, S.R. Daigle

Acquisition of data (provided animals, acquired and managed patients, provided facilities, etc.): C.T. Campbell, J.N. Haladyna, T. Yamauchi, K.M. Bernt

Analysis and interpretation of data (e.g., statistical analysis, biostatistics, computational analysis): C.T. Campbell, J.N. Haladyna, D.A. Drubin, T.M. Thomson, N.J. Waters, R.A. Copeland, S.J. Blakemore, K.M. Bernt, S.R. Daigle

Writing, review, and/or revision of the manuscript: C.T. Campbell, J.J. Smith, R.A. Copeland, S.J. Blakemore, K.M. Bernt, S.R. Daigle

Administrative, technical, or material support (i.e., reporting or organizing data, constructing databases): M.J. Maria

Study supervision: R.A. Copeland, S.J. Blakemore, K.M. Bernt, S.R. Daigle

Acknowledgments

The authors thank John Obenauer and Yuhong Ning for their help with the bioinformatics analyses.

The costs of publication of this article were defrayed in part by the payment of page charges. This article must therefore be hereby marked *advertisement* in accordance with 18 U.S.C. Section 1734 solely to indicate this fact.

Received October 18, 2016; revised February 3, 2017; accepted April 14, 2017; published OnlineFirst April 20, 2017.

References

1. Hess JL. MLL: a histone methyltransferase disrupted in leukemia. Trends Mol Med 2004;10:500–7.
2. Krivtsov AV, Armstrong SA. MLL translocations, histone modifications and leukaemia stem-cell development. Nat Rev Cancer 2007;7:823–33.

3. Slany RK. The molecular biology of mixed lineage leukemia. Haematologica 2009;94:984–93.
4. Neff T, Armstrong SA. Recent progress toward epigenetic therapies: the example of mixed lineage leukemia. Blood 2013;121:4847–53.
5. Muntean AG, Hess JL. The pathogenesis of mixed-lineage leukemia. Annu Rev Pathol 2012;7:283–301.
6. Milne TA, Briggs SD, Brock HW, Martin ME, Gibbs D, Allis CD, et al. MLL targets SET domain methyltransferase activity to hox gene promoters. Mol Cell 2002;10:1107–17.
7. Nakamura T, Mori T, Tada S, Krajewski W, Rozovskaia T, Wassell R, et al. ALL-1 is a histone methyltransferase that assembles a supercomplex of proteins involved in transcriptional regulation. Mol Cell 2002;10: 1119–28.
8. Bitoun E, Oliver PL, Davies KE. The mixed-lineage leukemia fusion partner AF4 stimulates RNA polymerase II transcriptional elongation and mediates coordinated chromatin remodeling. Hum Mol Genet 2007;16:92–106.
9. Mueller D, Garcia-Cuellar MP, Bach C, Buhl S, Maethner E, Slany RK. Misguided transcriptional elongation causes mixed lineage leukemia. PLoS Biol 2009;7:e1000249.
10. Okada Y, Feng Q, Lin Y, Jiang Q, Li Y, Coffield VM, et al. hDOT1L links histone methylation to leukemogenesis. Cell 2005;121:167–78.
11. Bernt KM, Zhu N, Sinha AU, Vempati S, Faber J, Krivtsov AV, et al. MLL-rearranged leukemia is dependent on aberrant H3K79 methylation by DOT1L. Cancer Cell 2011;20:66–78.
12. Guenther MG, Lawton LN, Rozovskaia T. Aberrant chromatin at genes encoding stem cell regulators in human mixed-linkage leukemia. Genes Dev 2008;22:3403–8.
13. Krivtsov AV, Feng Z, Lemieux ME, Faber J, Vempati S, Sinha AU, et al. H3K79 methylation profiles define murine and human MLL-AF4 leukemias. Cancer Cell 2008;14:355–68.
14. Milne TA, Martin ME, Brock HW, Slany RK, Hess JL. Leukemogenic MLL fusion proteins bind across a broad region of the Hox a9 locus, promoting transcription and multiple histone modifications. Cancer Res 2005;65: 11367–74.
15. Monroe SC, Jo SY, Sanders DS, Basrur V, Elenitoba-Johnson KS, Slany RK, et al. MLL-AF9 and MLL-ENL alter the dynamic association of transcriptional regulators with genes critical for leukemia. Exp Hematol 2010; 39:77–86.e1-5.
16. Nguyen AT, Taranova O, He J, Zhang Y. DOT1L, the H3K79 methyltransferase, is required for MLL-AF9-mediated leukemogenesis. Blood 2011;117:6912–22.
17. Thiel AT, Blessington P, Zou T, Feather D, Wu X, Yan J, et al. MLL-AF9-induced leukemogenesis requires coexpression of the wild-type Mll allele. Cancer Cell 2010;17:148–59.
18. Feng Q, Wang H, Ng HH, Erdjument-Bromage H, Tempst P, Struhl K, et al. Methylation of H3-lysine 79 is mediated by a new family of HMTases without a SET domain. Curr Biol 2002;12:1052–8.
19. Steger DJ, Lefterova MI, Ying L, Stonestrom AJ, Schupp M, Zhuo D, et al. DOT1L/KMT4 recruitment and H3K79 methylation are ubiquitously coupled with gene transcription in mammalian cells. Mol Cell Biol 2008;28:2825–39.
20. Deshpande AJ, Deshpande A, Sinha AU, Chen L, Chang J, Cihan A, et al. AF10 regulates progressive H3K79 methylation and HOX gene expression in diverse AML subtypes. Cancer Cell 2014;26:896–908.
21. Daigle SR, Olhava EJ, Therkelsen CA, Majer CR, Sneeringer CJ, Song J, et al. . Selective killing of mixed lineage leukemia cells by a potent small-molecule DOT1L Inhibitor. Cancer Cell 2011;20:53–65.
22. Nguyen AT, Zhang Y. The diverse functions of Dot1 and H3K79 methylation. Genes Dev 2011;25:1345–58.
23. Chen L, Deshpande AJ, Banka D, Bernt KM, Dias S, Buske C, et al. Abrogation of MLL-AF10 and CALM-AF10-mediated transformation through genetic inactivation or pharmacological inhibition of the H3K79 methyltransferase Dot1l. Leukemia 2013;27:813–22.
24. Deshpande AJ, Chen L, Fazio M, Sinha AU, Bernt KM, Banka D, et al. Leukemic transformation by the MLL-AF6 fusion oncogene requires the H3K79 methyltransferase Dot1l. Blood 2013;121:2533–41.
25. Daigle SR, Olhava EJ, Therkelsen CA, Basavapathruni A, Jin L, Boriack-Sjodin PA, et al. Potent inhibition of DOT1L as treatment for MLL-fusion leukemia. Blood 2013;122:1017–25.
26. Stein EM, Garcia-Manero G, Rizzieri DA, Tibes R, Berdeja JG, Jongen-Lavrencic M, et al. A phase 1 study of the DOT1L inhibitor, pinometostat (EPZ-5676), in adults with relapsed or refractory leukemia: safety, clinical activity, exposure and target inhibition. Blood 2015;126:2547.
27. Daver N, Cortes J, Ravandi F, Patel KP, Burger JA, Konopleva M, et al. Secondary mutations as mediators of resistance to targeted therapy in leukemia. Blood 2015;125:3236–45
28. Holohan C, Van Schaeybroeck S, Longley DB, Johnston PG. Cancer drug resistance: an evolving paradigm. Nat Rev Cancer 2013;13:714–26.
29. Zhang W, Gao C, Konopleva M, Chen Y, Jacamo RO, Borthakur G, et al. Reversal of acquired drug resistance in FLT3-mutated acute myeloid leukemia cells via distinct drug combination strategies. Clin Cancer Res 2014;20:2363–74.
30. Minson KA, Smith CC, DeRyckere D, Libbrecht C, Lee-Sherick AB, Huey MG, et al. The MERTK/FLT3 inhibitor MRX-2843 overcomes resistance-conferring FLT3 mutations in acute myeloid leukemia. JCI Insight 2016;1: e85630.
31. Wander SA, Levis MJ, Fathi AT. The evolving role of FLT3 inhibitors in acute myeloid leukemia: quizartinib and beyond. Ther Adv Hematol 2014;5:65–77.
32. Zhang W, Gao C, Konopleva M, Chen Y, Jacamo RO, Borthakur G, et al. Reversal of acquired drug resistance in FLT3-mutated acute myeloid leukemia cells via distinct drug combination strategies. Clin Cancer Res 2014;20:2363–74.
33. Kindler T, Lipka DB, Fischer T. FLT3 as a therapeutic target in AML: still challenging after all these years. Blood 2010;116:5089–102.
34. Weisberg E, Sattler M, Ray A, Griffin JD. Drug resistance in mutant FLT3-positive AML. Oncogene 2010;29:5120–34.
35. Gibaja V, Shen F, Harari J, Korn J, Ruddy D, Saenz-Vash V, et al. Development of secondary mutations in wild-type and mutant EZH2 alleles cooperates to confer resistance to EZH2 inhibitors. Oncogene 2016; 35:558–66.
36. Baker T, Nerle S, Pritchard J, Zhao B, Rivera VM, Garner A, Gonzalvez F. Acquisition of a single EZH2 D1 domain mutation confers acquired resistance to EZH2-targeted inhibitors. Oncotarget 2015;6:32646–55.
37. Drexler HG, Quentmeier H, MacLeod RA. Malignant hematopoietic cell lines: in vitro models for the study of MLL gene alterations. Leukemia 2004;18:227–32.
38. Olhava EJ, inventor; Epizyme, Inc, assignee. Methods of synthesizing substituted purine compounds. United States patent US 14/210,888. 2015 Nov 3.
39. Simon N, Dailly E, Combes O, Malaurie E, Lemaire M, Tillement JP, et al. Role of lipoproteins in the plasma binding of SDZ PSC 833, a novel multidrug resistance-reversing cyclosporin. Br J Clin Pharmacol 1998; 45:173–5.
40. Gilmartin AG, Bleam MR, Groy A, Moss KG, Minthorn EA, Kulkarni SG, et al. GSK1120212 (JTP-74057) is an inhibitor of MEK activity and activation with favorable pharmacokinetic properties for sustained in vivo pathway inhibition. Clin Cancer Res 2011;17:989–1000.
41. Blake JF, Burkard M, Chan J, Chen H, Chou KJ, Diaz D, et al. Discovery of (S)-1-(1-(4-Chloro-3-fluorophenyl)-2-hydroxyethyl)-4-(2-((1-methyl-1H-pyrazol-5-yl)amino)pyrimidin-4-yl)pyridin-2(1H)-one (GDC-0994), an extracellular signal-regulated kinase 1/2 (ERK1/2) inhibitor in early clinical development. J Med Chem 2016;59:5650–60.
42. King AJ, Arnone MR, Bleam MR, Moss KG, Yang J, Fedorowicz KE, et al. Dabrafenib; preclinical characterization, increased efficacy when combined with trametinib, while BRAF/MEK tool combination reduced skin lesions. PLoS One 2013;8:e67583.
43. Callaghan R, Luk F, Bebawy M. Inhibition of the multidrug resistance P-glycoprotein: time for a change of strategy? Drug Metab Dispos 2014;42: 623–31.
44. Ivy SP, Olshefski RS, Taylor BJ, Patel KM, Reaman GH. Correlation of P-glycoprotein expression and function in childhood acute leukemia: a children's cancer group study. Blood 1996;88:309–18.
45. Callaghan R, Crowley E, Potter S, Kerr ID. P-glycoprotein: so many ways to turn it on. J Clin Pharmacol 2008;48:365–78.
46. Sui H, Fan ZZ, Li Q. Signal transduction pathways and transcriptional mechanisms of ABCB1/Pgp-mediated multiple drug resistance in human cancer cells. J Int Med Res 2012;40:426–35.
47. Leith CP, Kopecky KJ, Godwin J, McConnell T, Slovak ML, Chen IM, et al. Acute myeloid leukemia in the elderly: assessment of multidrug resistance (MDR1) and cytogenetics distinguishes biologic subgroups with

remarkably distinct responses to standard chemotherapy. A Southwest Oncology Group Study. Blood 1997;89:3323–9.
48. Guerci A, Merlin JL, Missoum N, Feldmann L, Marchal S, Witz F, et al. Predictive value for treatment outcome in acute myeloid leukemia of cellular daunorubicin accumulation and P-glycoprotein expression simultaneously determined by flow cytometry. Blood 1995;85:2147–53.
49. Campos L, Guyotat D, Archimbaud E, Calmard-Oriol P, Tsuruo T, Troncy J, et al. Clinical significance of multidrug resistance P-glycoprotein expression on acute nonlymphoblastic leukemia cells at diagnosis. Blood 1992;79:473–6.
50. Mayer U, Wagenaar E, Dorobek B, Beijnen JH, Borst P, Schinkel AH. Full blockade of intestinal P-glycoprotein and extensive inhibition of blood-brain barrier P-glycoprotein by oral treatment of mice with PSC833. J Clin Invest 1997;100:2430–6.
51. Gottesman MM, Fojo T, Bates SE. Multidrug resistance in cancer: role of ATP-dependent transporters. Nat Rev Cancer 2002;2:48–58.
52. Tidefelt U, Liliemark J, Gruber A, Liliemark E, Sundman-Engberg B, Juliusson G, et al. P-Glycoprotein inhibitor valspodar (PSC 833) increases the intracellular concentrations of daunorubicin in vivo in patients with P-glycoprotein-positive acute myeloid leukemia. J Clin Oncol 2000;18:1837–44.
53. Fracasso PM, Westervelt P, Fears CL, Rosen DM, Zuhowski EG, Cazenave LA, et al. Phase I study of paclitaxel in combination with a multidrug resistance modulator, PSC 833 (Valspodar), in refractory malignancies. J Clin Oncol 2000;18:1124–34.
54. Advani R, Fisher GA, Lum BL, Hausdorff J, Halsey J, Litchman M, et al. A phase I trial of doxorubicin, paclitaxel, and valspodar (PSC 833), a modulator of multidrug resistance. Clin Cancer Res 2001;7:1221–9.
55. Roberts PJ, Der CJ. Targeting the Raf-MEK-ERK mitogen-activated protein kinase cascade for the treatment of cancer. Oncogene 2007;26:3291–310.
56. Zhang L, Strong JM, Qiu W, Lesko LJ, Huang SM. Scientific perspectives on drug transporters and their role in drug interactions. Mol Pharm 2006;3:62–9.
57. Chen Z, Shi T, Zhang L, Zhu P, Deng M, Huang C, et al. Mammalian drug efflux transporters of the ATP binding cassette (ABC) family in multidrug resistance: A review of the past decade. Cancer Lett 2016;370:153–64.
58. Riva L, Luzi L, Pelicci PG. Genomics of acute myeloid leukemia: the next generation. Front Oncol 2012;2:40.
59. Welch JS, Link DC. Genomics of AML: clinical applications of next-generation sequencing. ASH Education Program Book 2011;2011:30–5.
60. Papaemmanuil E, Gerstung M, Bullinger L, Gaidzik VI, Paschka P, Roberts ND, et al. Genomic classification and prognosis in acute myeloid leukemia. N Engl J Med 2016;374:2209–21.
61. Scholl C, Fröhling S, Dunn IF, Schinzel AC, Barbie DA, Kim SY, et al. Synthetic lethal interaction between oncogenic KRAS dependency and STK33 suppression in human cancer cells. Cell 2009;137:821–34.